JOURNAL OF PROPULSION AND POWER
Vol. 23, No. 4, July–August 2007

Technical Notes

TECHNICAL NOTES are short manuscripts describing new developments or important results of a preliminary nature. These Notes should not exceed 2500 words (where a figure or table counts as 200 words). Following informal review by the Editors, they may be published within a few months of the date of receipt. Style requirements are the same as for regular contributions (see inside back cover).

Axial Temperature Behavior of a Heat Exchanger Tube for Microwave Thermal Rockets

Alexander R. Bruccoleri*
Dartmouth College, Hanover, New Hampshire 03755
Kevin L. G. Parkin†
NASA Ames Research Center,
Moffett Field, California 94035
and
M. Barmatz‡
Jet Propulsion Laboratory,
California Institute of Technology,
Pasadena, California 91109

DOI: 10.2514/1.27847

Nomenclature

A	=	channel cross sectional area
$c_p(T)$	=	specific heat at constant pressure
D	=	channel diameter
$H(T)$	=	convective heat transfer coefficient
$k(T)$	=	fluid thermal conductivity
l	=	channel length
$\dot{m}$	=	mass flow rate
Nu	=	Nusselt number
P	=	inner channel perimeter
Pr	=	Prandtl number
$q''_{\text{convection}}$	=	convective heat flux
$q''_{\text{radiation}}$	=	radiation heat flux
q_{tube}	=	heat rate
Re	=	Reynolds number
T_m	=	mean fluid temperature
T_w	=	wall temperature
T_∞	=	ambient temperature
u_m	=	mean fluid velocity
ε	=	emissivity
$\mu(T)$	=	viscosity
ρ	=	density
σ	=	Stephan–Boltzmann constant

Received 18 October 2006; revision received 23 February 2007; accepted for publication 6 April 2007.

*Undergraduate Student, Engineering Sciences; currently Associate Researcher, Small Spacecraft Office, NASA Ames Research Center, Moffett Field, CA 94035; Alexander.R.Bruccoleri.07@Alum.Dartmouth.org. Student Member AIAA.

†Postdoctoral Scientist, Small Spacecraft Office.

‡Principal Member of Technical Staff, Thermo and Cryogenic Engineering, 4800 Oak Grove Drive, M/S 79-24.

I. Introduction

MICROWAVE thermal rockets bypass the chemical propulsion performance limitation by using an external energy source and an onboard heat exchanger (see Fig. 1). The first detailed concept for beamed energy propulsion used ground-based lasers and was proposed by Kantrowitz in 1972 [1]. Many variants of laser propulsion exist, with the laser heat exchanger design proposed by Kare [2] being the most similar to the microwave thermal rocket. Kare proposes a collection of diode lasers on the ground as a power source. In contrast, a phased array at 140 GHz is planned for the microwave thermal rocket. In both concepts, other power sources are possible without changing the basic physics of the heat exchanger.

With microwave thermal propulsion, the highest exhaust velocities for a given temperature occur with hydrogen as a monopropellant. With fluid temperatures around 1800 K, a specific impulse of 700 s can be reached, which enables a single stage to orbit vehicles with substantial payload fractions [3]. The first technical challenge is the development of a heat exchanger capable of transferring microwave energy into a heated gas. Such a heat exchanger can be thought of as a two-phase process; the heat exchanger walls absorb microwave energy, and then convectively transfers the heat into the fluid. The fluid can be thought of as a coolant moving through a tube that increases temperature as it moves along. The wall will have a similar temperature profile except it will be slightly warmer than the mean fluid temperature at any given point along the axis. An experimental study of the temperature profile of the tube wall's outer surface is the focus of this paper.

In place of a free space microwave beam, a 1 KW magnetron coupled to a resonant cavity is used for these experiments, to create a strong microwave field in an enclosed environment. A dielectric tube is placed axially in the cavity, and the working fluid flows through the tube. In earlier work, silicon carbide was suggested to be an ideal heat exchanger material [3]; however mullite, an aluminum oxide/silicon dioxide composite, is used instead for most of the experiments because it is readily available. Both materials have similar qualitative absorptive properties when heated. However silicon carbide is superior due to its higher melting point. Helium is the working fluid for these experiments because it is noncombustible and therefore easier to use in a laboratory environment.

II. Objective and Problem Statement

The operational heat exchangers planned for flight vehicles are designed to transfer roughly 30 MW/m^2 of microwave energy to heat in a working fluid. The smallest vehicles are anticipated to carry 100 kg into orbit using a heat exchanger roughly 1 m across. Furthermore, the working fluid must be heated to above 1800 K, which means the vast amount of energy is transferred via convection because radiation accounts for roughly 1 MW/m^2. The heat radiated is equal to

$$q''_{\text{radiation}} = \varepsilon\sigma\left(T_w^4 - T_\infty^4\right) \tag{1}$$

The current design calls for a collection of square channels roughly a millimeter across to be placed in parallel to form the heat exchanger.

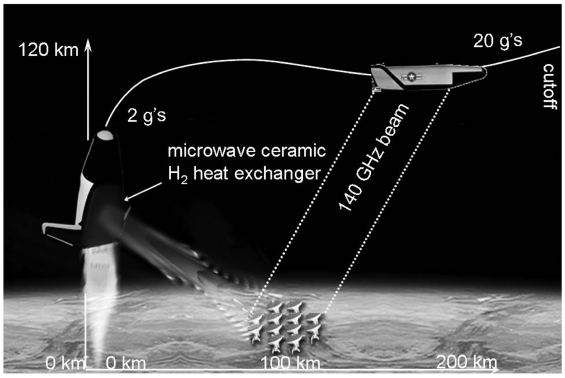

Fig. 1 Artist concept of microwave thermal propulsion.

It is assumed that each channel can be treated independently, and as the gas gets heated from one end to the other, the surface will have an axial temperature gradient. The goal for the current laboratory setup is to simulate one of these tubes, to observe the temperature profile along the tube with gas flow, and to compare the temperature profile to that of a tube without gas. Once the temperature profile is understood, arbitrary temperatures can be reached by changing the length of tube and the microwave field intensity. The temperature variation along the tube wall is the important parameter, and as a result one can choose a working fluid, tube shape, and material almost arbitrarily in the laboratory.

III. Basic Heat Exchanger Calculations

The microwave thermal rocket calls for the transmission of roughly 30 MW/m^2 into hydrogen though the channel wall. The hydrogen would be turbulent and the majority of the heat transfer would be convective. A preliminary analysis is presented here to convey the dynamics for such a heat exchanger. The defining parameters for a turbulent heat exchanger are the Nusselt and Reynolds numbers. The elementary heat exchanger assumes a collection of channels roughly 1 mm in diameter with a Reynolds number of approximately 10^5. The Nusselt number for circular flow is empirically [4]

$$Nu = 0.023(Re)^{0.8}(Re)^{1/3} \tag{2}$$

and the Reynolds number is

$$Re = \frac{\rho u_m D}{\mu(T)} \tag{3}$$

This can be rearranged to give

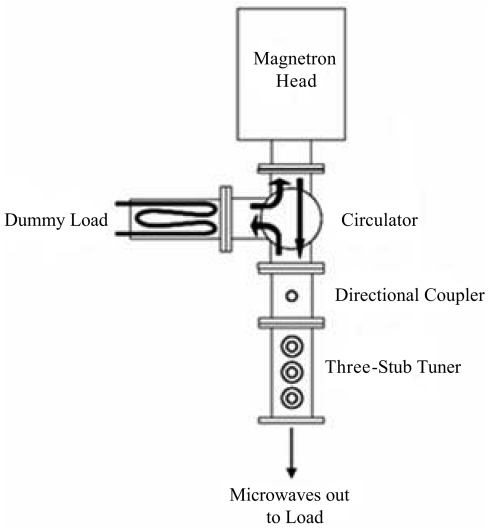

Fig. 2 Microwave circuit.

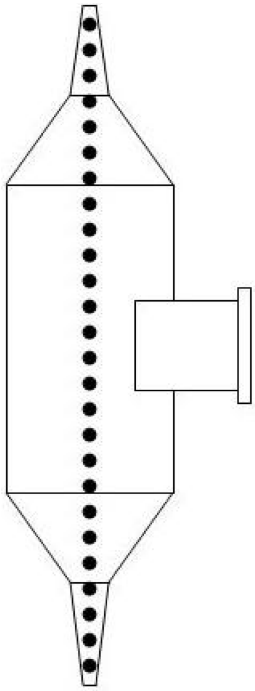

Fig. 3 Microwave cavity (not to scale).

$$Re = \frac{\dot{m}D}{A\mu(T)} \tag{4}$$

Because

$$\dot{m} = \rho A u_m \tag{5}$$

the Nusselt number is defined as

$$Nu(T) = \frac{H(T)D}{k(T)} \tag{6}$$

Setting Eqs. (2) and (6) equal, and rearranging terms provides the following expression for the convective heat transfer coefficient

$$H(T) = \frac{k(T)}{D} 0.023(Re)^{0.8}(Re)^{1/3} \tag{7}$$

where the Prandtl number is defined as,

$$Re = \frac{\mu(T)c_p(T)}{k(T)} \tag{8}$$

The net convective heat transfer flux is

$$q'' = H(T)(T_w - T_m) \tag{9}$$

This means at 1000 K the convective heat transfer coefficient will be 5.7×10^5 W/(m$^2 \cdot$ K). To reach a heat flux of 30 MW/m^2, the difference between the wall temperature and the mean fluid temperature will be 50 K. This does oversimplify the problem as the temperature dependent parameters and friction become significant; however this is a first order example of what the microwave thermal thruster will be. Furthermore, the heat exchanger is only a meter long and the temperature gradient is thus 1800 K/m, assuming a linear temperature profile and an exit temperature of 1800 K.

In the laboratory, the temperature gradient is a measurable value that confirms heat transfer into the fluid. Based on the mass flow rate and tube dimensions, the Reynolds numbers in the laboratory are 110, 220, and 275, which are well below the critical Reynolds number of 2300 for the onset of turbulence [4]. In the laminar regime, the temperature gradient can be shown to be [4]

$$\frac{\mathrm{d}T_m}{\mathrm{d}x} = \frac{q''P}{\dot{m}c_p} = \frac{P}{\dot{m}c_p}H(T)(T_w - T_m) \tag{10}$$

Using Eq. (10), the qualitative observation of the temperature gradient is completed in addition to a comparison of the measured temperature gradient and the gradient calculated using the heat flux measured. This is of importance because the mean fluid temperature can be obtained if the gradient is well understood.

IV. Experimental Apparatus

The experiments are performed in a resonant cavity powered by a 1 KW magnetron. Based off prior experiments, this apparatus produces a field intensity in excess of 3 MV/m and can therefore break the atmosphere down into a plasma. The system is modeled as a microwave transmission line, and the three stub tuner is used to match the impedance of the source and load [5]. (See Figs. 2 and 3 for a diagram of the circuit and cavity.) The net power entering the cavity is measured as the difference between the magnetron forward power and the reflected power, as measured by a microwave diode. The circuit and cavity are water cooled, and the reflected microwaves are absorbed into a dummy load after being redirected via a microwave circulator. The mullite tube is placed along the axis of the cavity. Gas enters the tube from the bottom, and an electronic mass flow controller controls the flow rate. The tube temperature is measured with an optical pyrometer mounted to a linear actuator, and the optics is focused on the tube through the holes in the cavity.

V. Experimental Procedure

The experiment first heats the tube to thermal runaway to establish a stable heating zone, and then the helium is passed through the tube. As the mullite heats, its dielectric loss increases, enabling it to absorb more microwave energy. At roughly 700 K, the tube reaches thermal runaway, a condition where it absorbs microwaves more strongly as the tube becomes warmer until it either melts or radiates the energy away. When thermal runaway takes place, it is very clear to the operator because the microwave energy strongly heats the mullite tube, and the reflected power drops off exponentially. See Fig. 4 for a sample output of what the operator sees during thermal runaway.

The heating of alumina and silicon carbide is due to Joule heating, a result of valence electrons that are elevated to a nearly free state at higher temperatures. (This process is different from the heating of water in a kitchen microwave, which heats up from molecular vibrations that resonate near 2.45 GHz.)

The magnetron forward power, three stub tuner, reflected power diode, mass flow controller, linear actuator, and pyrometer are controlled using a single LabView program. The equipment is turned on and the magnetron power is maintained at 75 W. The system is then tuned to minimize the reflected power, and the equipment is also checked for microwave leaks. The holes in the cavity leaked approximately 3 mW/cm^2, and any leakage above 5 mW/cm^2 is not permitted. During tuning, the tube is removed, and if the reflected power spikes, the operator verifies that the tube is indeed absorbing energy. The forward power is then raised to 250 W, and a bright glowing tube visually confirms thermal runaway. The tube temperature profile is obtained using the pyrometer, and then the helium flow is activated. The tube temperature profile is then obtained once the glowing region and reflected power stabilize. The equipment is turned off completing the experiment. (See Tables 1 and 2 for a summary of the equipment and experimental parameters.)

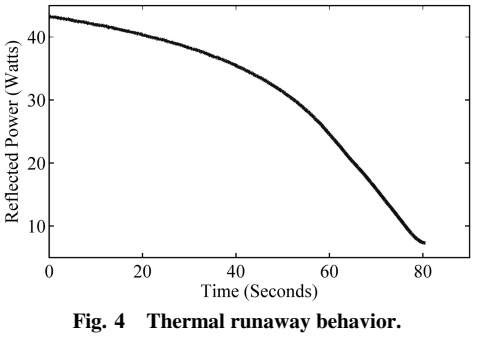

Fig. 4 Thermal runaway behavior.

VI. Experimental Analysis

The raw data are filtered to remove data points that indicate the pyrometer is not observing the tube. As the pyrometer moves up and down the tube, the temperature profile has a sinusoidal component accounted for by the cavity blocking the field of view. To remove that artifact, only the local maximum of each region is plotted. The gradient is then calculated by taking the difference in temperature between each point and dividing it by the distance to yield Figs. 5a–5c.

The heat flux is calculated to a very rough approximation due to a limited ability to take data within the resonant cavity. Given the tube temperature, convective heat transfer coefficient, ambient surroundings, and emissivity, the heat flux is calculated using

$$q''_{\text{tube}} = q''_{\text{convective}} + q''_{\text{radiation}} = H(T)(T_w - T_\infty) + \varepsilon\sigma\left(T_w^4 - T_\infty^4\right) \tag{11}$$

The net heat flow into the tube is therefore

$$q_{\text{tube}} = \int_0^l q''_{\text{tube}}(x)P\,\mathrm{d}x \tag{12}$$

The convective heat transfer coefficient is roughly 30 W/(m$^2 \cdot$ K) and the emissivity is obtained from a polynomial curve [6]. The heat flux out of the tube is calculated for cases with and without the helium flow, and the difference is assumed to be convection into the fluid. This is a rough approximation, because the electric field is coupled to the temperature profile of the tube. Specifically, the resistivity of the dielectric will decrease as it heats, and the electric field is coupled to the resistivity of the tube [3]. The glowing region of the tube moves upward with fluid flow and the field therefore changes. As a result, the electric field cannot be assumed constant in each test; however it is assumed constant for the reasoning set forth by this paper.

The temperature gradient calculated using Eq. (10) qualitatively follows a similar graph with the measured gradient. The temperatures are observed for half the tube, because the tube cools down due to the weakening electric field. The fluid could still be at a lower mean temperature than the tube wall, even if the tube is cooling, hence the only observed portion of the tube is where the field is either constant or increasing.

VII. Results

Figures 5a–5c show the temperature profile of the tube along with the temperature gradient. Sharp gradients are accounted for by abrupt changes of the electric field strength in the cavity [3]. The temperature profile becomes smoother as gas flow increases; specifically, sharp temperature changes tend to get smoother. This makes sense, because in Eq. (10), the amount of energy absorbed into the gas is proportional to the difference between the mean fluid and wall temperature. This can most easily be seen in the flow with 256 W input power.

Figure 6 shows the heat flux through the tube without gas flow. In this laboratory setup, the Reynolds numbers and convective heat transfer coefficients are small, and a higher heat flux would have melted the tube. If the system were full scale for use in a launch vehicle, it would require a heat flux roughly 100 times as high. It would therefore need a much higher Reynolds number flow to absorb the energy.

Figures 7a–7c show the temperature gradient of the tube compared with the gradient calculated using the inferred heat flux. The results match within 50% for the input power of 216 W, which is acceptable considering the assumptions made for the heat flux. The other graphs also show qualitative similarities between the calculated and measured gradients.

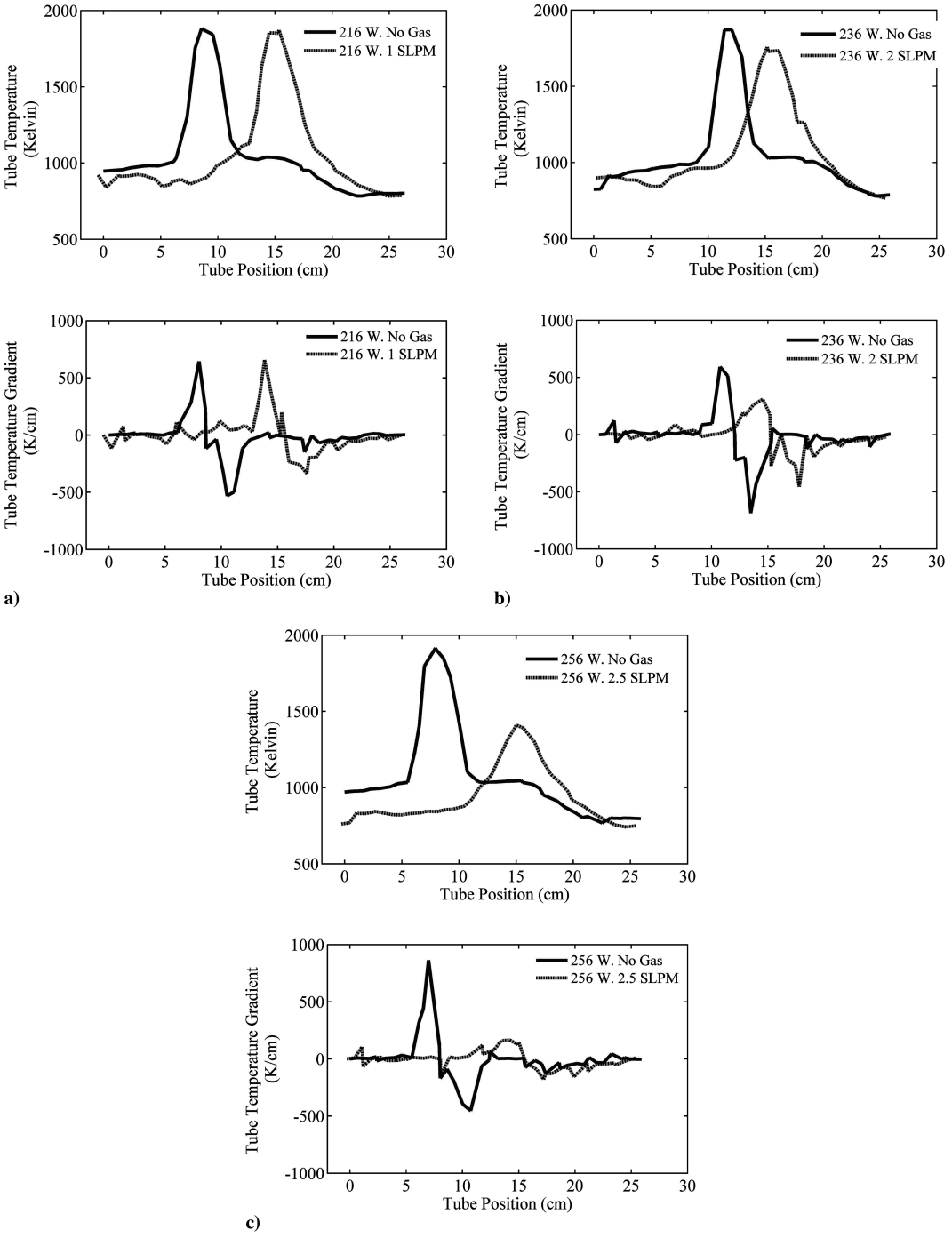

Fig. 5 Temperature profile of tube.

Figure 8, respectively, shows the mullite without and with helium flow at roughly 250 W. It is clear that the glowing region is farther up the tube with gas than without gas. It is also less bright. The far right image shows a high grade (99.8%) alumina rod wrapped with silicon carbide thread at roughly 800 W. (That is a proof of concept experiment that demonstrates the cavity is capable of coupling energy into silicon carbide.)

VIII. Error Analysis

The error analysis was performed using first order error propagation theory. The partial derivatives were calculated for each function with respect to each variable that had an associated error. Each of those derivatives was multiplied by the error, and the absolute value of those terms was summed to obtain the net error. The total temperature error consisted of both a random and a systematic error; we used a random error of 2 K and a systematic of 10 K. These values were estimated using the high precision specifications given for the pyrometer. For gradient calculations, the random error is the only relevant parameter, because any systematic error is eliminated

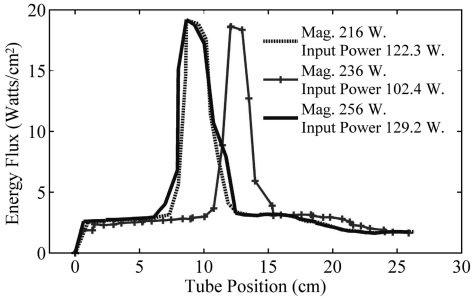

Fig. 6 Heat flux along the tube.

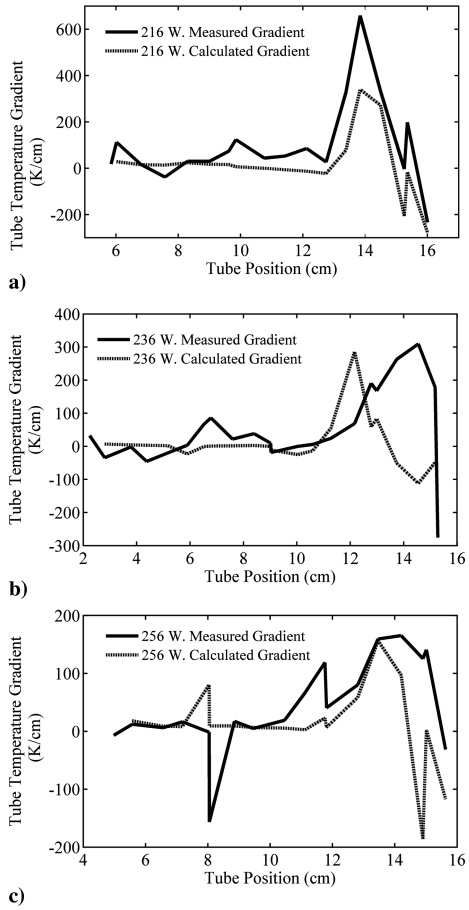

Fig. 7 Measured and calculated temperature gradient.

during subtraction. However for the heat flux calculation, the accuracy error was taken into account, because the partial derivative of Eq. (11) with respect to temperature is a function of the temperature.

The result of the analysis is an error approximately 5 K/cm for the measured gradient. It should be noted that a few points along the curve were ignored because they were artifacts of the choice of valid data points. Because the raw data from the pyrometer were filtered for a local maximum, it was possible to have two points with abnormally close position. When this occurred the difference in position was small and the random temperature error remained constant, which lead to a large error. Roughly two of these points were found in each data set and they were removed from the calculations.

The error for the calculated gradient was roughly half the error for the measured gradient, 3 K/cm. This error is small compared with the gradient in all graphs which was on the order of at least 10^2 K/cm.

Lastly the error for the heat flux along the tube was calculated as a percent value. It is reported this way because the heat flux varied roughly an order of magnitude along the rod, the error also varied with a similar profile. The percent error was roughly constant at approximately 6.5%, which was acceptable given the assumptions made for calculating heat flux. (See Table 3 for quantified error analysis.)

IX. Discussion and Future Recommendations

In general, the results are acceptable as the working fluid clearly affected the gradient of the tube temperature. The temperature gradient using the inferred heat flux is within 50% of the measured gradient for a magnetron power of 216 W, which suggest that energy is stably transferred into the fluid. It is important to understand the temperature gradient for future heat exchanger development because it is related to the working fluid temperature. The most desirable

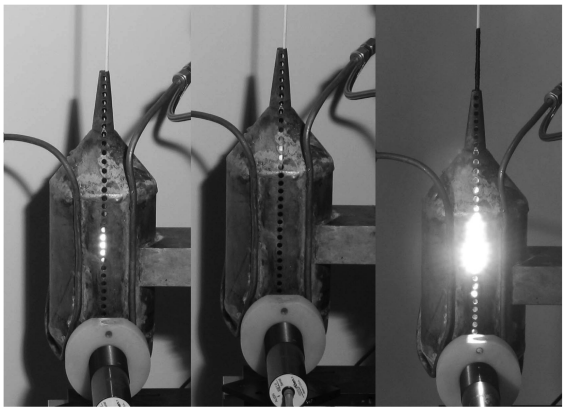

Fig. 8 Tube without gas, with gas, and with silicon carbide coating.

improvement for future research is a microwave field that does not change axially along the tube or with the tube temperature. (This would be a free space beam using a dish to focus the microwaves onto the heat exchanger.) The operation of the cavity is interesting in this regard; during the initial heating of a tube without gas flow, there is a region roughly 4 in. long in the center that starts to glow. As it gets hot, a region 2 in. long glows bright orange and that condition is stable for at least 5 min. Once the gas is released through the tube, the glowing region both moves up the tube and stabilizes, or it moves up and terminates with thermal runaway. To optimize heat transfer the operator must use the maximum flow rate without terminating thermal runaway. This always involves a shift in the location of the tube's glowing region. The microwave field must therefore be

Table 1 Summary of essential equipment

Item	Specification
Magnetron	Astex 50–800 W forward power forward power, 2.45 GHz
Pyrometer 1	Luxtron accufiber M100 C, fiber optic 950 nm single frequency
Mass flow controller	Omega FMA 1600A, 0–20 SLPM, 1–10 atm pressure

Table 2 Experimental parameters

Tube parameters	
Length	60.7 ± 3 cm
Inner diameter	0.156 ± 0.008 cm
Outer diameter	0.318 ± 0.016 cm
Material	Mullite (omega ORM-11618-24)
Cavity parameters	
Inner diameter	9.85 ± 0.05 cm
Taper end diameter	2 ± 1 cm
Choke end diameter	0.7 ± 0.1 cm
Main cylindrical section length	14.7 ± 0.1 cm
Left taper length	5.2 ± 0.1 cm
Right taper length	5.2 ± 0.1 cm
Choke length (both ends)	5.65 ± 0.1 cm
Drive point length	25.527 ± 1 mm (60% of waveguide height; measured)
Offset from center of cylindrical main section.	$(0.075 \pm 0.075$ cm) toward the right/outlet; measured
Flow parameters	
Gas	Helium
Mass flow rate	$1, 2, 2.5 \pm 0.01$ SLPM
Inlet Reynolds number	110, 220, 275
Tube energy parameters	
Tube temperature range	$(700–1950) \pm 2$ K
Magnetron forward power	$216, 236, 256 \pm 15$ W
Linear actuator range	$(0–270) \pm 0.1$ mm

Table 3 Summary of average error

Figure	Error
5a–5c: Temperature	Random error $\pm$ **2** K
5a–5c: Temperature gradient without gas flow	Input (216, 236, 256) W, respective net error (**4.24**, **3.31**, **2.32**) K/cm
5a–5c: Measured temperature gradient with gas flow	Input (216, 236, 256) W, respective net error (**4.76**, **8.46**, **3.68**) K/cm
6: Heat flux along the tube	Input (216, 236, 256) W, respective net percent error (**6.78**%, **6.71**%, **6.95**%)
7a–7c: Calculated temperature gradient with gas flow	Input (216, 236, 256) W, respective net error (**2.97**, **2.28**, **4.95**) K/cm

independent of the tube temperature profile to better demonstrate that the shift is caused solely by the fluid flow.

With the current laboratory setup, two improvements could be implemented for future work. First, a control system could to be written to control the tuning of the cavity. The system can creep out of thermal runaway, specifically with gas flow. The operator has to manually keep the reflected power at a minimum to avoid this consequence. Software should be able to handle this situation.

Second, the cavity also could be remade to improve the pyrometer's view of the tube. The metal between the holes interferes with the operation of the pyrometer and the data are filtered. To increase the resolution of the filtered data, long slits roughly 2 cm could be cut into the cavity instead of holes. This will cause microwave leakage and a Faraday cage must be used if long slits are cut into the cavity.

The next experiments should try to obtain a clearer contrast in tube temperature profiles between tubes with and without gas flow. A uniform profile is desirable without gas flow and a linear temperature profile is obtained with gas flow. Ideally, one would like to see a tube at room temperature at the gas inlet and a linear progression to over 1500 K at the exit. This would clearly demonstrate that the gas causes a well-understood gradient. That experiment would be the precursor to a larger system where the exit temperature of the gas is increased to over 1800 K.

X. Conclusions

Stable heating of helium gas was demonstrated and analyzed with a mullite tube in a microwave resonant cavity. The temperature profile of the tube and its gradient was measured and the tube heat flux was calculated. Using the heat flux inferred from the data, the temperature gradient along the tube with helium flow was calculated and compared qualitatively with the measured gradient. The error in the instruments was small, and the calculated error propagation was much less than the deviations observed in the figures. The simplified models used to calculate heat flux are the main error source. Future work needs to decouple the microwave field from the tube temperature profile to obtain better results. A proof of concept for thermal runaway was also demonstrated using silicon carbide string wrapped around an alumina rod. That experiment was interesting; however repeatable results were unobtainable. Future work involving doping silicon carbide with vanadium to change the dielectric loss would be useful toward developing a microwave thermal thruster, and the current laboratory setup is suitable for such an endeavor [7].

Acknowledgments

A portion of this work was carried out under a contract with the National Aeronautics and Space Administration. The authors would like to thank Karen Bradford, Simon Worden, Orlando Santos, Steven Zornetzer, and Robert Bruccoleri for their support; and Kurtis Long, Jim Ross, James Bell, Davis Yaste, and Greg Zilliac for their help in the laboratory.

References

[1] Kantrowitz, A., "Propulsion to Orbit by Ground-Based Lasers," *Astronautics and Aeronautics*, Vol. 10, No. 5, 1972, p. 74.

[2] Kare, J. T., "Laser Powered Heat Exchanger Rocket for Ground-to-Orbit Launch," *Journal of Propulsion and Power*, Vol. 11, No. 3, 1995, pp. 535–543.

[3] Parkin, K. L. G., "The Microwave Thermal Thruster and Its Application to the Launch Problem," Doctorate Thesis, Department of Aeronautics, California Inst. of Technology, 2006, pp. 25, 55, 60–68, 111–145.

[4] Incropera, F. P., and DeWitt, D. P., "Internal Flow," *Fundamentals of Heat and Mass Transfer*, 5th ed., Wiley, New York, 2002, pp. 466–506.

[5] Barmatz, M., Iny, O., Yiin, T., and Khan, I., "Vibration Method for Tracking the Resonant Mode and Impedance of a Microwave Cavity," *Ceramic Transactions*, Vol. 59, May 1995, pp. 167–174.

[6] Goodson, C. C., "Simulation of Microwave Heating of Mullite Rods," Master's Thesis, Virginia Polytechnic Institute and State University, 1997, pp. 29–41.

[7] Gradinaru, G., Sudarshan, T. S., Gradinaru, S. A., Mitchell, W., and Hobgood, H. M., "Electrical Properties of High Resistivity 6H–SiC Under High Temperature/High Field Stress," *Applied Physics Letters*, Vol. 70, No. 6, 1997, pp. 735–737.

G. Spanjers
Associate Editor